Theory for the cyclotron resonance of holes in strained asymmetric Ge-SiGe quantum wells

R. Winkler,* M. Merkler, T. Darnhofer, and U. Rössler
Institut für Theoretische Physik, Universität Regensburg, D-93040 Regensburg, Germany
(Received 13 July 1995)

We present calculations of hole Landau levels, cyclotron masses, and far-infrared spectra for strained asymmetric p-type Ge-Si_xGe_{1-x} quantum wells in a perpendicular magnetic field in order to interpret recent experimental results by Engelhardt *et al.* [Solid State Electron. **37**, 949 (1994)]. Self-consistent hole subband calculations are combined with calculations of the Landau levels using a 6×6 $\mathbf{k}\cdot\mathbf{p}$ Hamiltonian for the topmost Γ_8 and Γ_7 bulk valence bands. Our results are in very good agreement with the experimental data. Taking into account the coupling to the split-off band turns out to be important. The complex spectra of hole Landau levels in strained quantum wells remind one of the well known quantum resonance spectra of bulk p-type Ge under uniaxial stress.

I. INTRODUCTION

Since the first successful growth of Si_xGe_{1-x} layers on a Si substrate using molecular-beam epitaxy (MBE),[1] this technique has been developed with the objective to open the possibility of band structure engineering to Si-based technology.[2,3] This endeavor is motivated by the fact that, compared with metal-oxide-semiconductor structures of the standard Si-SiO_2 technology, MBE grown interfaces have higher perfection, allowing for much higher mobilities of the confined carriers, i.e., faster devices. The price for this advantage is the lattice mismatch between Si and Ge, which limits the pseudomorphic growth of strained layers to critical thicknesses of a few atomic layers for the pure materials. Using Si_xGe_{1-x} alloys, however, the critical thickness can be increased to several hundred angstroms.[4] The high quality of recently grown heterostructures, quantum wells (QW's), and superlattices using Si, Ge, and Si_xGe_{1-x} has been demonstrated in a series of optical and transport experiments.[2,5–10]

The starting point of our investigations are experiments by Engelhardt *et al.*[7,8] on cyclotron resonance (CR) of holes in strained Ge layers confined between Si_xGe_{1-x} barriers of different composition x. The lower barrier is a graded Si_xGe_{1-x} buffer layer[3] grown on a Si substrate with a final Ge content of $(1-x)=0.7$. The upper Si_xGe_{1-x} barrier is δ doped with a spacer between the doping layer and the two-dimensional (2D) hole gas in the Ge well. The structures were overgrown with a Si cap layer. All relevant parameters for the two samples C1072 and C1116 of Refs. 7 and 8 are given in Table I. The experimental CR spectra for the two samples, measured at $T=4.2$ K with a Fourier spectrometer, are reproduced in Fig. 1. From these spectra one can extract the CR energies $\hbar\omega_c^*$ or cyclotron masses $m_c^*=eB/\omega_c^*$, which uncover the complex structure of the Landau level spectrum of holes in strained QW's. The different Si contents in the two barriers and the δ-doping layer in the upper barrier result in an inversion asymmetry of the QW, which removes the spin degeneracy. Thus even the single peak observed in the ''classical'' limit of low magnetic fields consists of a spin-split doublet.[8] With increasing magnetic field the doublet splits into several components whose evolution is characteristic for the sample (hole concentration, width of the QW) as the Fermi energy is moved to Landau levels with lower quantum numbers. In bulk p-type semiconductors with uniaxial stress applied in the direction of **B**, these Landau levels are known to be quite irregularly spaced as a consequence of the complex valence-band structure.[11–13] The corresponding cyclotron transitions have been called ''quantum resonances.''[12] The experimental data of Ref. 8 provide evidence of such quantum resonances in strained 2D hole systems.

The theory of Landau levels for 2D hole systems has been developed for p-type inversion layers at the interface of GaAs-$Al_xGa_{1-x}As$ heterostructures[14–17] in order to describe experimental data by Störmer *et al.*[18] First the subband problem is solved self-consistently for $\mathbf{B}=\mathbf{0}$. Then the $\mathbf{B}=\mathbf{0}$ Hartree potential is used for the calculation of Landau levels. Most of these calculations use Luttinger's 4×4 $\mathbf{k}\cdot\mathbf{p}$ model[14,15,17] for the topmost fourfold bulk valence band Γ_8 of light holes (LH's) and heavy holes (HH's). Only in Ref. 16 was the split-off (SO) valence band Γ_7 taken into account

TABLE I. Parameters of the two samples C1072 and C1116 of Refs. 7 and 8.

Sample C1072	Sample C1116	Parameter
		upper SiGe barrier
0.5	0.6	Ge content
5	5	δ-doping (10^{12} cm^{-2})
75	100	spacer width (Å)
		Ge well
75	168[a]	width (Å)
1.78	1.10	N_s (10^{12} cm^{-2})
		lower SiGe barrier
0.7	0.7	Ge content

[a]The well width of sample C1116 of 168 Å was obtained by TEM measurements. It deviates from the nominal width of 125 Å (Refs. 7 and 8).

with a 6×6 $\mathbf{k}\cdot\mathbf{p}$ model. For undoped rectangular QW's calculations of Landau levels and matrix elements for interband optical transitions have been performed using a 6×6 $\mathbf{k}\cdot\mathbf{p}$ model, which includes the lowest conduction band.[19] All these studies yield fan charts of Landau levels evolving from each hole subband, which show a rather complex dependence on the magnetic field as a consequence of the coupling between LH and HH states, but failed to account for the experimental results of Ref. 18.

In a recent work by Wong *et al.*[10] CR data on *p*-type strained layer Si_xGe_{1-x}-Si heterostructures were presented. An interpretation of the main resonances was given by a 6×6 $\mathbf{k}\cdot\mathbf{p}$ model, assuming a rectangular subband potential without performing self-consistent calculations for the confined hole states.

In the present paper we use a 6×6 $\mathbf{k}\cdot\mathbf{p}$ Hamiltonian for Γ_8 and Γ_7 as in Ref. 16, taking into account the coupling to the SO band. In the application to Ge QW's between Si_xGe_{1-x} barriers it is important to consider also strain effects. Therefore, the $\mathbf{k}\cdot\mathbf{p}$ Hamiltonian is augmented by the strain Hamiltonian of Bir and Pikus.[20] The self-consistent subband calculations are performed for the $\mathbf{B}=\mathbf{0}$ case. In order to calculate the multicomponent envelope function we solve the coupled integral equations in k_z space by means of a quadrature method.[21] Then Landau levels are obtained by the same procedure, but by using the Hartree potential obtained for $\mathbf{B}=\mathbf{0}$ and replacing the 2D plane waves by oscillator states. We calculate cyclotron masses, dipole transition matrix elements, and the full far-infrared (FIR) absorption spectra, which allow direct comparison with all features in the complex experimental data of Fig. 1.

II. SELF-CONSISTENT SUBBAND CALCULATIONS FOR $B=0$

The starting point of our calculations for a 2D hole gas in a biaxially strained QW between asymmetric barriers (which may also be strained) is the 6×6 $\mathbf{k}\cdot\mathbf{p}$ Hamiltonian acting in the space of the Γ_8 and Γ_7 bulk valence-band states. Using as a basis the Bloch eigenstates $|JM\rangle$ with angular momentum $J=3/2$, $M=+3/2,+1/2,-1/2,-3/2$ for Γ_8 and $J=1/2$, $M=+1/2,-1/2$ for Γ_7, the Hamiltonian reads, in the magnetic-field-free case,

$$H_{6\times6}=E_v\otimes\mathbb{1}-H_{\mathbf{k}}-H_{\boldsymbol{\varepsilon}}. \tag{1}$$

Here E_v is the (position-dependent) valence-band edge and

$$H_{\mathbf{k}}=\begin{pmatrix} P+Q & S & R & 0 & -S/\sqrt{2} & -R\sqrt{2} \\ S^\dagger & P-Q & 0 & R & Q\sqrt{2} & S\sqrt{3/2} \\ R^\dagger & 0 & P-Q & -S & S^\dagger\sqrt{3/2} & -Q\sqrt{2} \\ 0 & R^\dagger & -S^\dagger & P+Q & R^\dagger\sqrt{2} & -S^\dagger/\sqrt{2} \\ -S^\dagger/\sqrt{2} & Q\sqrt{2} & S\sqrt{3/2} & R\sqrt{2} & P+\Delta_0 & 0 \\ -R^\dagger\sqrt{2} & S^\dagger\sqrt{3/2} & -Q\sqrt{2} & -S/\sqrt{2} & 0 & P+\Delta_0 \end{pmatrix}, \tag{2}$$

with

$$P=\frac{\hbar^2}{2m_0}\gamma_1(k_x^2+k_y^2+k_z^2), \tag{3a}$$

$$Q=\frac{\hbar^2}{2m_0}\gamma_2(k_x^2+k_y^2-2k_z^2), \tag{3b}$$

$$R=\frac{\hbar^2}{2m_0}(-\sqrt{3}/2)[(\gamma_2+\gamma_3)k_-^2+(\gamma_2-\gamma_3)k_+^2], \tag{3c}$$

$$S=\frac{\hbar^2}{2m_0}(-2\sqrt{3})\gamma_3 k_- k_z, \tag{3d}$$

where $k_\pm=k_x\pm ik_y$. The Hamiltonian $H_{\boldsymbol{\varepsilon}}$ due to the strain $\boldsymbol{\varepsilon}$ has the same form as $H_{\mathbf{k}}$ in Eq. (2), but with P and Q replaced by

$$P_{\boldsymbol{\varepsilon}}=-D_d(\varepsilon_{xx}+\varepsilon_{yy}+\varepsilon_{zz}), \tag{4a}$$

$$Q_{\boldsymbol{\varepsilon}}=\frac{1}{3}D_u(\varepsilon_{xx}+\varepsilon_{yy}-2\varepsilon_{zz}), \tag{4b}$$

and the other terms set equal to zero.[20] In $H_{6\times6}$ the z axis is the growth direction [001] and the biaxial strain is in the xy plane. Due to the layered structure the material specific parameters E_v, Δ_0, γ_1, γ_2, γ_3, D_d, and D_u as well as the components of the strain tensor $\boldsymbol{\varepsilon}$ depend on z. This requires the use of properly symmetrized expressions in order to maintain Hermiticity of $H_{6\times6}$.[21] The bulk valence-band parameters for Ge and Si are well known.[22] The corresponding parameters for Si_xGe_{1-x} are obtained by an interpolation scheme described in the Appendix. The valence-band offsets are taken from Ref. 23.

For biaxial strain and $k_\parallel=0$ the total Hamiltonian $H_{6\times6}$ is diagonal in the 4×4 block of the $J=3/2$ states and in the 2×2 block of the $J=1/2$ states. However, the LH and the SO states, having the same z component of angular momentum ($M=\pm1/2$), are coupled by terms proportional to Q. The z dependence of E_v and Δ_0 together with the strain-induced offsets define the carrier-free potential profiles of the layered structures; they are different for LH, HH, and SO states.

The samples of Refs. 7 and 8 are δ doped in the upper barrier with a spacer between the doping layer and the 2D hole gas. Investigations on δ-doped GaAs:Si have shown

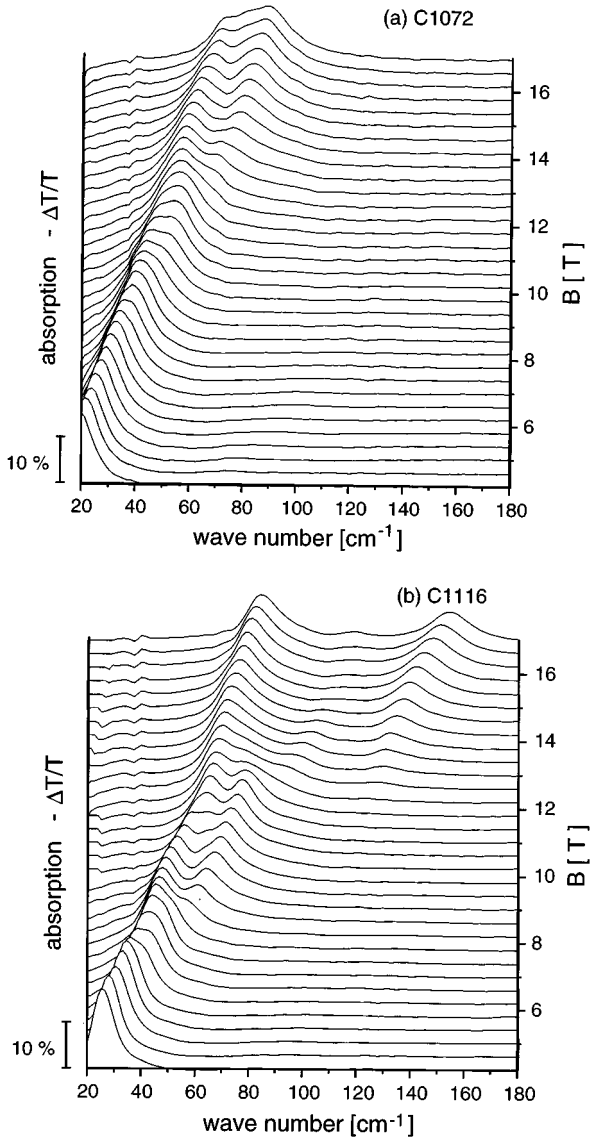

FIG. 1. Experimental cyclotron resonance spectra at different magnetic fields for the two samples (a) C1072 and (b) C1116 as specified in Table I. Taken from Refs. 7 and 8.

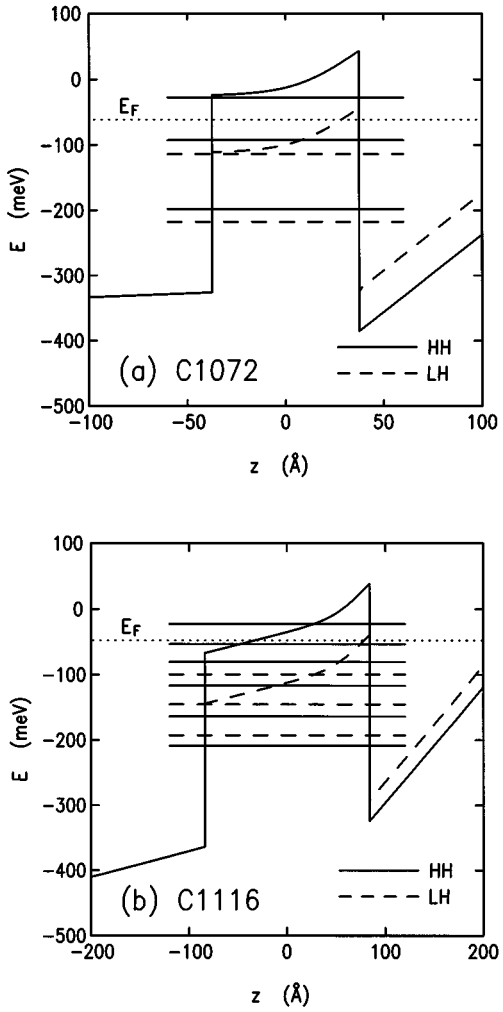

FIG. 2. Self-consistent potential profiles and hole subband energies at $k_\parallel = 0$ for the two samples (a) C1072 and (b) C1116. Due to the biaxial strain on the quantum well and on the upper barrier, different potential profiles result for heavy-holes (solid line) and light holes (dashed line).

that during the growth process the impurity atoms will diffuse and widths of the actual doping layers of up to 200 Å have been reported.[24] This has been considered in our self-consistent hole subband calculations by assuming several widths of the doping layer. It turns out that the calculated FIR spectra do not depend sensitively on this parameter.

The hole subbands are calculated for zero magnetic field by self-consistently solving $H_{6\times6}$ and the Poisson equation to obtain the Hartree potential, which is superimposed to the z-dependent band-edge energies. This is done by solving the coupled integral equations in k_z space using a quadrature method.[21,25] We apply the axial approximation by neglecting in Eq. (3c) the warping term proportional to $(\gamma_2 - \gamma_3)$. For the hole densities of the samples in Refs. 7 and 8 only the topmost HH subband is occupied. In Fig. 2 we show the self-consistently calculated potential profiles for the two samples together with the subband energies at $k_\parallel = 0$. We remark that for the topmost subband in the wider sample C1116 the probability of finding a hole in the lower barrier (in Fig. 2 the barrier on the left-hand side) is negligible. Therefore our calculations are rather insensitive with respect to the exact value of the width of the QW, which was somewhat uncertain for sample C1116.[7,8] The hole subband dispersion $\mathscr{E}(k_\parallel)$ is displayed in Fig. 3. Note the spin splitting of the subbands due to the asymmetry of the potential profile.[26] In Fig. 4 we show the density-of-states effective mass[25] of the topmost subband defined by

$$\frac{m^*(E)}{m_0} = \frac{1}{\pi}\frac{\hbar^2}{2m_0}\int \delta[E - \mathscr{E}(\mathbf{k}_\parallel)]\, d^2\mathbf{k}_\parallel . \tag{5}$$

In the experimental work[7,8] it was not well known whether the well material was fully strained according to the lattice mismatch between the well and barrier material or whether the well had relaxed to some extent. We found that our calculations depend rather sensitively on this effect, i.e., the relaxation tends to increase calculated CR masses. Therefore, we have used the strain as a fitting parameter. Best agreement was obtained when the strain had 90% (sample

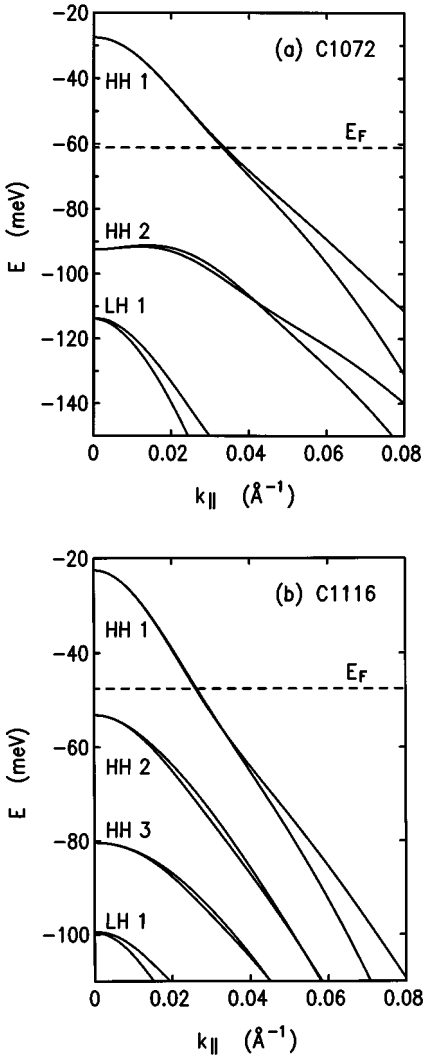

FIG. 3. Hole subband dispersion $\mathscr{E}(k_\parallel)$ for the two samples (a) C1072 and (b) C1116.

C1072) and 80% (sample C1116) of its value in a fully strained system. We note that it is reasonable to have the larger relaxation in the wider sample.

III. LANDAU LEVELS AND CYCLOTRON MASSES

We consider the magnetic field $\mathbf{B}=(0,0,B)$ applied parallel to the growth direction on the basis of the self-consistent calculations at $B=0$. We replace k_x, k_y by Landau raising and lowering operators[11–13]

$$a^\dagger=\frac{\lambda_c}{\sqrt{2}}(k_x+ik_y), \quad a=\frac{\lambda_c}{\sqrt{2}}(k_x-ik_y), \tag{6}$$

where $\lambda_c=\sqrt{\hbar/(eB)}$ is the cyclotron radius. In the axial approximation $H_{\mathbf{k}}$ becomes a 6×6 matrix operator in the form of Eq. (2) but with

$$P=\frac{\hbar^2}{2m_0}\gamma_1\left[\frac{2}{\lambda_c^2}\left(a^\dagger a+\frac{1}{2}\right)+k_z^2\right], \tag{7a}$$

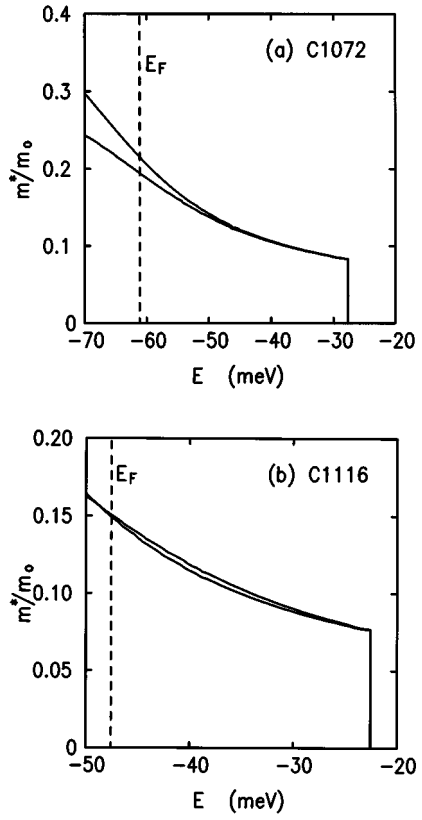

FIG. 4. Density-of-states effective mass of the topmost subband for the two samples (a) C1072 and (b) C1116.

$$Q=\frac{\hbar^2}{2m_0}\gamma_2\left[\frac{2}{\lambda_c^2}\left(a^\dagger a+\frac{1}{2}\right)-2k_z^2\right], \tag{7b}$$

$$R=\frac{\hbar^2}{2m_0}(-\sqrt{3}/2)(\gamma_2+\gamma_3)\frac{2}{\lambda_c^2}a^2, \tag{7c}$$

$$S=\frac{\hbar^2}{2m_0}(-2\sqrt{3})\gamma_3\frac{\sqrt{2}}{\lambda_c}ak_z. \tag{7d}$$

Zeeman terms are added in the diagonal and in the off-diagonal blocks coupling LH and SO states, which are weighted by the isotropic and anisotropic hole g factors κ and q, respectively. The matrix operator $H_{\mathbf{k}}$ is identical to the corresponding 6×6 block of the Hamiltonians of Ref. 13.

Due to the axial symmetry the total Hamiltonian $H_{6\times6}$ commutes with $\hat{F}=a^\dagger a+J_z$, which corresponds to the conservation of total angular momentum.[11–13,27] Therefore, we use a basis of spinors whose six components are products of envelope functions for the confined motion in z direction $\xi_j(z)$ and oscillator eigenstates for the in-plane motion $|n_j\rangle$ $(j=1,\ldots,6)$. In this basis the Hamiltonian falls into blocks for fixed eigenvalues $F=n_j+M_j$ of $\hat{F}$, where M_j is the z component of the angular momentum of the jth spinor component.[28] Each block, together with the self-consistent Hartree potential of Sec. II, is treated in the same way as the subband problem for $\mathbf{B}=\mathbf{0}$, i.e., the corresponding set of coupled integral equations is solved by a quadrature method.[21]

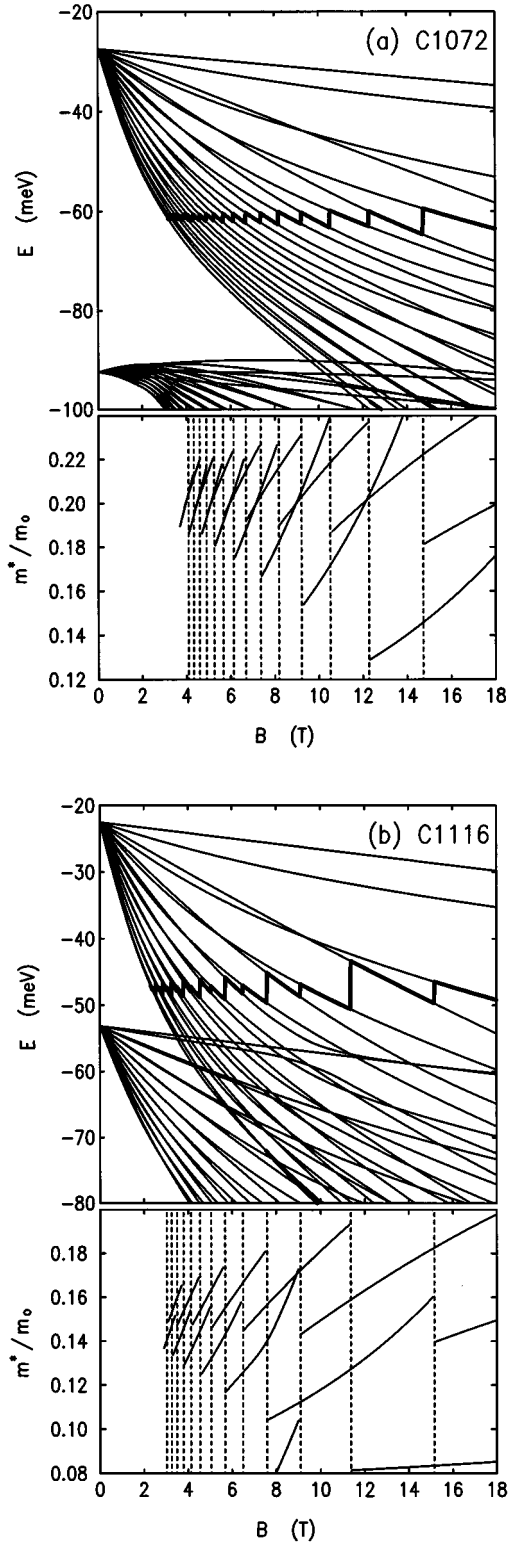

FIG. 5. Fan chart of Landau levels evolving from the two topmost heavy-hole subbands (upper parts) together with the Fermi energy (bold line), and corresponding cyclotron masses (lower parts) for the two samples (a) C1072 and (b) C1116.

In Fig. 5 we show for the two samples of Table I the fan chart of Landau levels evolving from the topmost HH subbands together with the Fermi energy E_F obtained from the hole density. From top to bottom the Landau levels belong to increasing n and $M=\pm 3/2$ (according to the dominant component of the eigenvectors) with spin down ($M=-3/2$) being the higher level at small magnetic fields. With increasing magnetic field the spin-split states tend to change their order. The spin splitting of the Landau levels is a consequence of the Zeeman splitting and the asymmetry of the Hartree potential.[14–17] The nonlinear dependence of the Landau levels on B corresponds to the nonparabolic dispersion $\mathscr{E}(k_\parallel)$ of the topmost HH subband (see Fig. 3).

From the fan chart of Fig. 5 we obtain cyclotron masses in the standard way by considering pairs of Landau levels (separated by $\hbar\omega_c^*$) between which dipole transitions are possible due to the occupation factors and the selection rule $\Delta F=+1$ for plus polarization of the circular polarized FIR radiation. With changing magnetic field the cyclotron mass $m_c^*=eB/\omega_c^*$ refers to different pairs of Landau levels as visualized in the lower parts of Fig. 5. For small magnetic fields (large filling factors) we find two spin-split cyclotron masses. As expected, for $B\to 0$ they are close to the values of m^*, which for the classical limit of large Landau level quantum numbers can be read from the density-of-states effective mass at E_F (see Fig. 4). With increasing magnetic field (decreasing filling factor) the transitions take place between Landau levels with smaller n, which show irregularities inherent with the top of the valence band.

In Ref. 29 we have presented some preliminary results on the same subject. There we used a simplified scheme for the numerical solution of the $\mathbf{B}\neq\mathbf{0}$ eigenvalue problem based on an expansion in terms of $\mathbf{B}=\mathbf{0}$ eigenstates. However, for high magnetic fields the shape of the spinor components $\xi_j(z)$ differs strongly from the shape of the nonvanishing $\xi_j(z)$ for $\mathbf{B}=\mathbf{0}$. Thus it would be necessary to use a basis consisting of a rather large number of $\mathbf{B}=\mathbf{0}$ eigenstates. However, the lower states in the QW are no longer discrete because due to the potential profile of these samples they couple to the continuum of barrier eigenstates. This makes it difficult to use these states as a basis set. In the present work we do not use such an expansion, but find the eigenstates by direct solution of the equations for $\mathbf{B}\neq\mathbf{0}$. This more accurate numerical solution yields considerably better agreement with experiment than the approach used in Ref. 29.

IV. ABSORPTION SPECTRA

We consider the absorption of FIR radiation with an electric-dipole field $\mathbf{E}=E_0\hat{\mathbf{e}}e^{i\omega t}$, where $\hat{\mathbf{e}}=(e_x,e_y,e_z)$ denotes the polarization vector. The transition probability between eigenstates $|s\rangle$ and $|t\rangle$ of $H_{6\times 6}$ of Sec. III with eigenenergies E_s and E_t is given by Fermi's golden rule[12]

$$W_{st}(\omega)=\frac{\pi e^2E_0^2}{2\hbar\omega^2}|\langle s|\hat{\mathbf{e}}\cdot\mathbf{v}|t\rangle|^2[\,\delta(E_{st}-\hbar\omega)+\delta(E_{st}+\hbar\omega)\,]. \tag{8}$$

Here $E_{st}=E_s-E_t$ and $\mathbf{v}=\partial H_{\mathbf{k}}/\hbar\partial\mathbf{k}$ is the velocity operator, which in the present case is a 6×6 matrix operator. Following Ref. 12 we obtain, for the matrix elements in Eq. (8),

$$\langle s|\hat{\mathbf{e}}\cdot\mathbf{v}|t\rangle=\frac{\lambda_c E_{ts}}{\hbar}\langle s|e_+a+e_-a^\dagger+e_z\lambda_c k_z|t\rangle, \tag{9}$$

where $e_\pm=(e_x\pm ie_y)/\sqrt{2}$.

The 2D absorption coefficient $\alpha(\omega)$ is defined as the energy absorbed per unit time and area divided by the energy flux of the radiation field, hence it is dimensionless. With the energy density of the radiation field $U=E_0^2/(8\pi)$ and n the index of refraction, the energy flux is ncU and we get

$$\alpha(\omega)=\frac{\hbar\omega N_L}{ncU}\sum_{s,t} f_s(1-f_t)W_{st}(\omega), \tag{10}$$

where $N_L=eB/(2\pi\hbar)$ is the degeneracy of the Landau levels per unit area and f_s and f_t are the occupation factors, which depend on the 2D hole concentration and on the magnetic field. We assume zero temperature. Finally, we obtain

$$\alpha(\omega)=\frac{2\pi}{n}\frac{e^2}{\hbar c}\sum_{s,t}(f_s-f_t)E_{ts}|\langle s|e_+a+e_-a^\dagger+e_z\lambda_c k_z|t\rangle|^2 \times\delta(E_{ts}-\hbar\omega). \tag{11}$$

For the present case of an electric-dipole field with circular polarization in the plus direction we have $e_-=e_z=0$. In our calculation the δ function in Eq. (11) is replaced by a Lorentzian broadening with the same phenomenological linewidth for all transitions. The best agreement with the experimental data is obtained for a linewidth of 0.7 meV.

The calculated spectra for the two samples C1072 and C1116 are shown in Fig. 6 and allow direct comparison with the experimental spectra of Fig. 1. All essential features of the experimental data are reproduced by our calculation: wavelength and magnetic-field dependence of the resonances, intensities of the absorption lines, and the characteristic differences between the two samples. A striking difference between the two samples is that for high magnetic fields up to 18 T the cyclotron transition $(F=0)\rightarrow(F=1)$ at wave numbers between 140 and 180 cm^{-1} becomes possible only for the sample C1116 with the lower 2D charge density. These results are in close agreement with the experimental data (see Fig. 1 of the present paper and Fig. 4 of Ref. 8), although the interpretation in Ref. 8 in terms of Landau levels of bulk Ge is not correct.

As already mentioned in Sec. II, the calculated FIR spectra of Fig. 6 are not very sensitive to the position and profile of the δ doping for a given hole concentration, and for the sample C1116 the spectra also do not depend on the assumed well width. However, for either sample the results change dramatically if calculated on the basis of the 4×4 Luttinger Hamiltonian: the cyclotron masses decrease, the crossing of the spin-split Landau levels shifts to higher magnetic fields, and the FIR resonances move up to 20 cm^{-1} towards higher energies. Thus taking into account the coupling to the SO band Γ_7 is essential for the agreement with the experimental data.

V. CONCLUSION

We have extended the existing theoretical concepts to describe Landau levels and FIR absorption of confined holes in order to describe recent experiments of Engelhardt *et al.*[7,8] on strained asymmetric p-type Ge-Si_xGe_{1-x} QW's. Our calculations reproduce all relevant features in the experimental spectra for the two different samples of Ref. 8. For this good agreement between theory and the experimental data, it was important to consider the effects of strain due to the lattice mismatch between Ge and Si_xGe_{1-x} and to use a 6×6 $\mathbf{k}\cdot\mathbf{p}$ Hamiltonian that includes the coupling between the Γ_8 and the Γ_7 band.

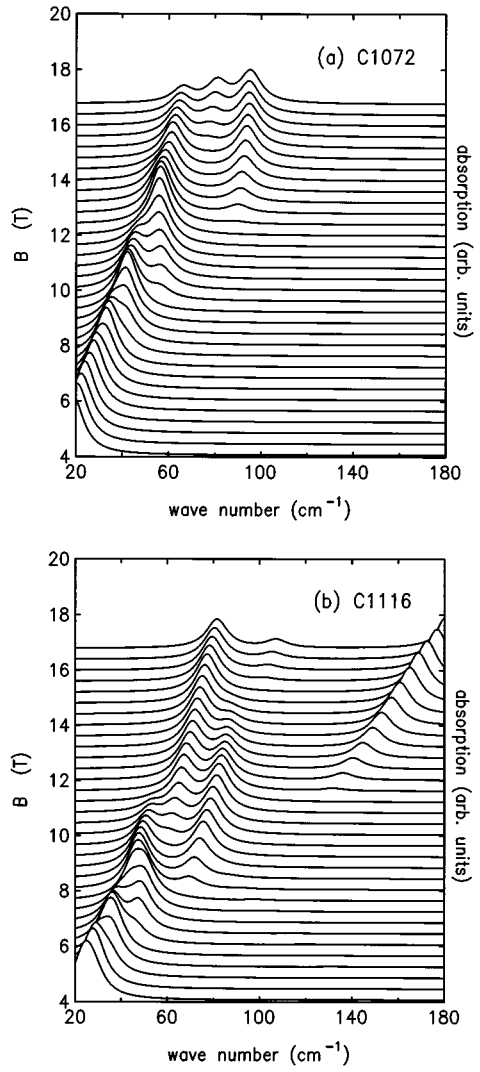

FIG. 6. Cylotron absorption spectra calculated from the Landau levels of Fig. 5, for the two samples (a) C1072 and (b) C1116. A phenomenological broadening of 0.7 meV is assumed for all transitions.

ACKNOWLEDGMENTS

We thank C. M. Engelhardt and co-workers at the Technische Universität München for providing their experimental data, for helpful discussions, and for a reading of this manuscript. Financial support from the Deutsche Forschungsgemeinschaft and from the Bayerische Forschungsstiftung (FOROPTO) is gratefully acknowledged.

APPENDIX: INTERPOLATION SCHEME FOR THE LUTTINGER PARAMETERS

Experimental values for the Luttinger parameters of Si_xGe_{1-x} bulk material do not exist in the literature.[22] From empirical pseudopotential calculations Rieger and Vogl[23] found a nonlinear dependence of the mass parameters on x.

Their results are in quantitative agreement with the well known data for Si but deviate significantly from the values for Ge. Therefore, we have used a nonlinear interpolation scheme along the concepts of Lawaetz,[30] which exactly reproduces the experimental values of the Luttinger parameters of both Si and Ge. The dominant contributions to these parameters derive from $\mathbf{k}\cdot\mathbf{p}$ couplings of the topmost valence band with the s and p antibonding conduction-band states with energy gaps E_0 and E_0', respectively. This allows the decomposition

$$\gamma_1=\frac{1}{3}\frac{E_p}{E_0}+\frac{2}{3}\frac{E_p'}{E_0'}+\overline{\gamma_1}, \tag{A1a}$$

$$\gamma_2=\frac{1}{6}\frac{E_p}{E_0}-\frac{1}{6}\frac{E_p'}{E_0'}+\overline{\gamma_2}, \tag{A1b}$$

$$\gamma_3=\frac{1}{6}\frac{E_p}{E_0}+\frac{1}{6}\frac{E_p'}{E_0'}+\overline{\gamma_3}, \tag{A1c}$$

$$\kappa=\frac{1}{6}\frac{E_p}{E_0}-\frac{1}{6}\frac{E_p'}{E_0'}+\overline{\kappa}, \tag{A1d}$$

where E_p, E_p' are (up to a factor $2/m_0$) the squared absolute values of the corresponding momentum matrix elements. Note that in Lawaetz's[30] notation $\overline{\gamma_1}$, $\overline{\gamma_2}$, $\overline{\gamma_3}$, and $\overline{\kappa}$ are not independent but can be expressed by two constants (G and H_2 in Ref. 30). Thus, using the well known Luttinger parameters and the gaps E_0 and E_0' for Si and Ge,[22] we can determine E_p, E_p', $\overline{\gamma_1}$, $\overline{\gamma_2}$, $\overline{\gamma_3}$, and $\overline{\kappa}$ from Eqs. (A1a)–(A1d) for $x=1$ and 0.

Regarding the x dependence, the interpolation is based on the following assumptions: we use a linear interpolation between the E_0 gaps of Si and Ge and follow Lawaetz[30] by scaling E_0' according to

$$E_0'(x)=E_0'(1)\left[\frac{a(x)}{a(1)}\right]^{-1.92}. \tag{A2}$$

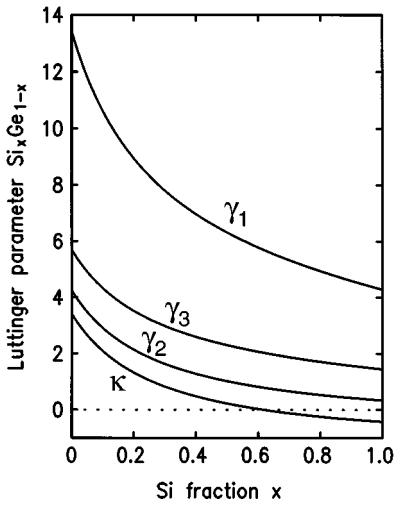

FIG. 7. Luttinger parameters for Si_xGe_{1-x} obtained from the parameters for Si and Ge using the interpolation formulas given in the Appendix.

The dependence of the lattice constant a on x is taken from Ref. 23:

$$a(x)=a(1)+0.200\ 36x(1-x)+[a(0)-a(1)](1-x)^2\ \text{Å}. \tag{A3}$$

We note that the momentum matrix elements are inversely proportional to the lattice constant. Therefore $E_p(x)$ and $E_p'(x)$ are obtained by scaling their values for Si with[30]

$$\delta(x)=\{1+1.23[D(x)-1]\}\left[\frac{a(1)}{a(x)}\right]^2. \tag{A4}$$

The values of $D(x)$, $\overline{\gamma_1}(x)$, $\overline{\gamma_2}(x)$, $\overline{\gamma_3}(x)$, and $\overline{\kappa}(x)$ are obtained by a linear interpolation between those of Si and Ge. The resulting x dependence of γ_1, γ_2, γ_3, and κ is shown in Fig. 7.

*Present address: Department of Physics and Astronomy, Vanderbilt University, Nashville, TN 37235.

[1] E. Kasper and H. J. Herzog, Appl. Phys. **8**, 199 (1975).
[2] G. Abstreiter, Phys. Scr. **T49**, 42 (1993).
[3] U. König, in *Festkörperprobleme (Advances in Solid State Physics XXXII)*, edited by U. Rössler (Pergamon-Vieweg, Braunschweig, 1992), p. 199.
[4] J. Brunner *et al.*, Thin Solid Films **222**, 27 (1992).
[5] G. Abstreiter, Solid State Commun. **92**, 5 (1994).
[6] J. P. Cheng, V. P. Kesan, D. A. Grützmacher, T. O. Sedgwick, and J. A. Ott, Appl. Phys. Lett. **62**, 1522 (1993).
[7] M. Aschauer, Diploma thesis, Technische Universität München, 1993 (unpublished).
[8] C. M. Engelhardt, D. Többen, M. Aschauer, F. Schäffler, G. Abstreiter, and E. Gornik, Solid State Electron. **37**, 949 (1994).
[9] V. I. Gavrilenko, I. N. Kozlov, O. A. Kuznetsov, M. D. Moldavskaya, V. V. Nikonorov, L. K. Orlov, and A. L. Chernov, Pis'ma Zh. Éksp. Teor. Fiz. **59**, 327 (1994) [JETP Lett. **59**, 348 (1994)]; Jpn. J. Appl. Phys. **33**, 2386 (1994).
[10] S. L. Wong, D. Kinder, R. J. Nicholas, T. E. Whall, and R. Kubiak, Phys. Rev. B **51**, 13499 (1995).
[11] J. M. Luttinger, Phys. Rev. **102**, 1030 (1956).
[12] J. C. Hensel and K. Suzuki, Phys. Rev. B **9**, 4219 (1974).
[13] H.-R. Trebin, U. Rössler, and R. Ranvaud, Phys. Rev. B **20**, 686 (1979); H. Mayer and U. Rössler, *ibid.* **44**, 9048 (1991).
[14] D. A. Broido and L. J. Sham, Phys. Rev. B **31**, 888 (1985).
[15] U. Ekenberg and M. Altarelli, Phys. Rev. B **32**, 3712 (1985); U. Ekenberg, Surf. Sci. **170**, 601 (1986).
[16] E. Bangert and G. Landwehr, Superlatt. Microstruct. **1**, 363 (1985).
[17] E. Bangert and G. Landwehr, Surf. Sci. **170**, 593 (1986).
[18] H. L. Störmer, Z. Schlesinger, A. Chang, D. C. Tsui, A. C. Gossard, and W. Wiegmann, Phys. Rev. Lett. **51**, 126 (1983).
[19] F. Ancilotto, A. Fasolino, and J. C. Maan, Phys. Rev. B **38**, 1788 (1988).
[20] G. L. Bir and G. E. Pikus, *Symmetry and Strain-Induced Effects in Semiconductors* (Wiley, New York, 1974), Chap. V.
[21] R. Winkler and U. Rössler, Phys. Rev. B **48**, 8918 (1993); Surf. Sci. **305**, 295 (1994).
[22] *Semiconductors. Intrinsic Properties of Group IV Elements and*

III-V, II-VI, and I-VII Compounds, edited by O. Madelung, Landolt-Börnstein, New Series, Group III, Vol. 22, Pt. a (Springer, Berlin, 1987).
[23] M. Rieger and P. Vogl, Phys. Rev. B **48**, 14 276 (1993).
[24] A. Zrenner, Appl. Phys. Lett. **55**, 156 (1989).
[25] R. Winkler, J. Phys. Condens. Matter **5**, 2321 (1993).
[26] G. Goldoni and A. Fasolino, Phys. Rev. Lett. **69**, 2567 (1992).
[27] D. A. Broido, A. Cros, and U. Rössler, Phys. Rev. B **45**, 11 395(1992).
[28] R. C. Pidgeon and R. N. Brown, Phys. Rev. **146**, 575 (1966).
[29] M. Merkler, R. Winkler, T. Darnhofer, and U. Rössler, in *Proceedings of the XIth International Conference on High Magnetic Fields in Semiconductor Physics, Boston, 1994*, edited by D. Heiman (World Scientific, Singapore, 1995), p. 624.
[30] P. Lawaetz, Phys. Rev. B **4**, 3460 (1971).